LA-UR 78-1891

TITLE: QUARKS AND GLUONS IN DEEP INELASTIC SCATTERING

AUTHOR(S): H. L. Anderson, L. C. Myrianthopoulos, and
H. S. Matis

SUBMITTED TO: XIX International Conference on High
Energy Physics, Tokyo, Japan, 8/23-30/78

By acceptance of this article for publication, the publisher recognizes the Government's (license) rights in any copyright and the Government and its authorized representatives have unrestricted right to reproduce in whole or in part said article under any copyright secured by the publisher.

The Los Alamos Scientific Laboratory requests that the publisher identify this article as work performed under the auspices of the USERDA.

Form No. 836
St. No. 2629
1/75

UNITED STATES
ENERGY RESEARCH AND
DEVELOPMENT ADMINISTRATION
CONTRACT W-7405-ENG. 36

E98 E398
FERMILAB-CONF-78-129-E

QUARKS AND GLUONS IN DEEP INELASTIC SCATTERING

H. L. Anderson,† L. C. Myrianthopoulos

The Enrico Fermi Institute, The University of Chicago,
Chicago, Illinois 60637

and

H. S. Matis

The University of California, Los Alamos Scientific Laboratory
Los Alamos, New Mexico 87545

ABSTRACT

We present a set of quark and gluon distribution functions obtained by fitting their n = 2, 4, 6 moments as determined from the corresponding measured Nachtmann moments from deep inelastic electron and muon scattering. A comparison of the calculated and measured F_2 values is given. These distributions are used to calculate F_2^ν and xF_3^ν for neutrino scattering and compared to recent data.

July 12, 1978

In the past few years the theory of quantum chromodynamics (QCD) has been shown to give a plausible account of a number of phenomena in high energy physics.[1] We refer, in particular, to the good account it gives of: 1) scale breaking in ep and μp deep inelastic scattering;[2-6] 2) $p + p \to \mu^+ + \mu^- + x$, the Drell-Yan process;[1,6,7] 3) high $p_\perp$ hadron-hadron scattering;[8-9] and 4) $\nu,\bar{\nu}$ inelastic scattering.[10] While none of these are conclusive enough to constitute a "proof" of QCD, they do provide an incentive to pursue possible applications of QCD more extensively and in greater detail. To this end it is important to have the quark and gluon momentum density functions; i.e., $q_i(x) = x\rho_i(x)$, where ρ_i is the quark density as a function of x.[6] The purpose of this note is to report an elementary determination of these density functions based on a knowledge of their n = 2, 4, 6 moments.

In a recent paper,[2] hereafter referred to as I, we showed how several of the moments of the structure functions $F_2(x,Q^2) \equiv \nu W_2(x,Q^2)$ could be evaluated by combining the existing electron and muon deep inelastic scattering data.[11,12] The corresponding quark and gluon moments were extracted through the use of the theory of asymptotic freedom.[13] This provided us with three moments for each constituent with which three parameters of a suitable momentum distribution function could be determined. We chose momentum densities in the form $q_i(x) = (a_i + b_i x)(1 - x)^{r_i}$, where x is the momentum of the constituent expressed as a fraction of the nucleon mass. We worked with a four-flavor, three-color model but considered that the contribution of the charmed quarks was negligible. Thus, the index i runs through four values, up, down, and strange quarks, and gluons. Our functional

FERMILAB-CONF-78-129-E

form is similar to that used by previous authors.[4-6] However, because it is somewhat arbitrary and does not have a sound theoretical basis, it cannot be expected to give reliable results outside the range of the data used to extract the moments.

The quark and gluon moments are defined, for up quarks, by

$$\langle U(Q^2)\rangle_n \equiv \int_0^1 x^{n-2}[u(x,Q^2) + \bar{u}(x,Q^2)]dx \qquad (1)$$

where u and $\bar{u}$ are the momentum densities of the quarks and anti-quarks, respectively, per unit momentum interval, in units of the nuclear mass; and similarly for the d, s, and c quarks; for gluons

$$\langle G(Q^2)\rangle_n = \int_0^1 x^{n-2}\, g(x,Q^2)dx \qquad (2)$$

where Q^2 is the square of the four-momentum transfer and $x = Q^2/2M\nu$ with ν the energy transferred to the nucleon in the laboratory system and M its rest mass.

In I we obtained the values of the quark and gluon moments at $Q_o^2 = 10\ \text{GeV}^2$, given in Table I. the Q^2 variation of the moments is given in terms of four coefficients, M_+ and M_- for the singlet terms and M_{NS}^P and M_{NS}^N for the non-sinhglet terms as follows:

$$\langle U(Q^2) + C(Q^2)\rangle_n = \tfrac{9}{5}[M_+(n,Q^2) + M_-(n,Q^2)] + 3M_{NS}^P(n,Q^2) \qquad (3a)$$

$$\langle D(Q^2) + C(Q^2)\rangle_n = \tfrac{9}{5}[M_+(n,Q^2) + M_-(n,Q^2)] + 3M_{NS}^N(n,Q^2) \qquad (3b)$$

$$\langle S(Q^2) - C(Q^2)\rangle_n = -3[M_{NS}^P(n,Q^2) + M_{NS}^N(n,Q^2)] \qquad (3c)$$

$$\langle G(Q^2)\rangle_n = \alpha_+^n M_+(n,Q^2) + \alpha_-^n M_-(n,Q^2) \qquad (3d)$$

with

$$M_+(n,Q^2) = M_+(n,Q_o^2)e^{-\lambda_+^n s} \tag{3e}$$

$$M_-(n,Q^2) = M_-(n,Q_o^2)e^{-\lambda_-^n s} \tag{3f}$$

$$M_{NS}^P(n,Q^2) = M_{NS}^P(n,Q_o^2)e^{-\lambda_{NS}^n s} \tag{3g}$$

$$M_{NS}^N(n,Q^2) = M_{NS}^N(n,Q_o^2)e^{-\lambda_{NS}^n s} \tag{3h}$$

and

$$s = \ell n[\ell n(Q^2/\Lambda^2)/\ell n(Q_o^2/\Lambda^2)] \quad . \tag{3i}$$

The λ's and α's are given explicitly by the theory of asymptotic freedom. In I we used the values for a three-color, four-flavor model. In Table II we give the values of the M's for n = 2, 4, 6 as determined in I for $Q_o^2 = 10$ GeV^2.

Using Eqs. (3), the quark and gluon moments for any value of Q^2 can be computed. However, the results become suspect outside the range $3.0 \leq Q^2 \leq 50.0$ GeV^2 of the data used in the analysis. Moreover, the approximations of the theory leave additional doubts about the results for values of Q^2 near the lower end of the range.

In evaluating the distribution functions from these moments we tried various functions. These gave rather similar results, except in the regions of small x, below the range of the data. We checked our solutions by using them to calculate $F_2(x,Q^2)$ according to the simple parton model,

$$F_2^p(x) = \frac{4}{9}[u(x) + \bar{u}(x)] + \frac{1}{9}[d(x) + \bar{d}(x)] + \frac{1}{9}[s(x) + \bar{s}(x)] \tag{4a}$$

$$F_2^N(x) = \frac{1}{9}[u(x) + \bar{u}(x)] + \frac{4}{9}[d(x) + \bar{d}(x)] + \frac{1}{9}[s(x) + \bar{s}(x)] \quad . \tag{4b}$$

for the proton and neutron, respectively. The Q^2 dependence of these functions is not shown explicitly but is implied. Here, and in what follows, we take the contribution of the c quarks to be negligible.

Among the functional forms we studied, the ones that gave the best fit to the proton and deuteron data are,

$$[u(x) + \bar{u}(x)] = (a_u + b_u x)(1-x)^{r_u} \tag{5a}$$

$$[d(x) + \bar{d}(x)] = (a_d + b_d x)(1-x)^{r_d} \tag{5b}$$

$$[s(x) + \bar{s}(x)] = a_s(1-x)^{r_s} \tag{5c}$$

$$g(x) = a_g(1-x)^{r_g} \quad . \tag{5d}$$

Note that we restricted the usual polynomial form in $(1-x)$ to one term only, but left the value of the exponent as a free parameter. In future work we intend to introduce more terms by utilizing the n = 3 and 5 moments as well.

Values of the coefficients at different values of Q^2 are shown in Table III. In Figs. 1, 2 and 3 we show the distribution of quarks and gluons at $Q^2 = 3.25$, 7.0, and 20.0 GeV^2, respectively. Although the functions

$u(x)$, etc. are well behaved as $x \to 0$, the functions $u(x)/x$, etc. are divergent and we have not extended our plots below $x = 0.05$.

Our results are consistent with the conditions

$$\int_0^1 [u(x) - \bar{u}(x)]\frac{dx}{x} = 2$$

and

$$\int_0^1 [d(x) - \bar{d}(x)]\frac{dx}{x} = 1$$

as required in parton theory to give the electric charge of the proton and neutron correctly. To evaluate these integrals we set $\bar{u}(x) = \bar{d}(x) = \bar{s}(x) = s(x)$, in accordance with the usual assumption about the production of the sea of quark, anti-quark pairs. The contribution to these integrals from $0.05 \leq x \leq 1.0$ is 1.10 and 0.32, respectively (for $Q^2 = 20$ GeV^2). Thus, a large contribution from the region $x \leq 0.05$ is called for and an appropriate function would have to be chosen to satisfy these integral conditions as well as the condition[7] $u(x) \to d(x)$ as $x \to 0$. In this report we make no proposals for the region $x \leq 0.05$.

In Figs. 4 and 5 we show the up quark and gluon momentum distributions $u(x)$ and $g(x)$, respectively, as a function of Q^2. The progressive peaking of these distributions at low x as Q^2 increases is clearly shown. This is the expected behavior in the theory of asymptotic freedom that gives rise to the scale breaking.

In Figs. 6-10 we show the fit of the hydrogen data to $F_2^p(x,Q^2)$ for $Q^2 = 3.25$, 9, 12.5, and 22.5 GeV^2 respectively, and for the deuteron data to $\frac{1}{2}[F_2^p(x,Q^2) + F_2^N(x,Q^2)]$ for $Q^2 = 12.5$ GeV^2. Here the values of F_2 have been evaluated assuming $R = 0.25$, constant throughout the full range of x.

This may not be a good assumption in general, and in the resonance region in particular. Moreover, in the resonance region we cannot expect a good fit unless we include higher moments than $n = 6$. On the whole, however, the fits are remarkably good considering that systematic errors of $\sim 7\%$ are not included in the error bars.

We show the fit in another way by plotting, in Figs. 11-15, $x^2F_2(x)$ to show the weighting used in obtaining the $n = 4$ moment. The deviations in the resonance region at large x are made more evident here. They become even more evident in Figs. 16-20 in the plots of $x^4F_2(x)$ corresponding to the $n = 6$ weighting. We think these plots give a fair picture of how well our quark distributions can be relied upon.

As a further check of our quark distribution functions, we used them to calculate the structure functions obtained from the neutrino scattering data.[10] Again we assume $c(x) \equiv \bar{c}(x) \equiv 0$ and write the structure function for the nucleon following Karliner and Sullivan,[14]

$$\begin{aligned} F_2^{\nu}(x,Q^2) = (1+R^{\nu}) \Big(& \Big\{ [u(x,Q^2) + d(x,Q^2) + \bar{u}(x,Q^2) + \bar{d}(x,Q^2)] \\ & + 2\eta_c\theta(yE-W_c)s(\xi_c,Q^2) \Big\} \cos^2(\theta_c) \\ & + \Big\{ [\bar{u}(x,Q^2) + \bar{d}(x,Q^2) + 2s(x,Q^2)] \\ & + \eta_c\theta(yE-W_c)(d(\xi_c,Q^2) + u(\xi_c,Q^2)) \Big\} \sin^2(\theta_c) \Big) \end{aligned} \qquad (6)$$

and

$$xF_3^{\nu}(x,Q^2) = \Big\{u(x,Q^2) + d(x,Q^2) - \bar{u}(x,Q^2) - \bar{d}(x,Q^2)$$
$$+ 2\theta(yE - W_c)\,\frac{1}{\eta_c}\,s(\xi_c,Q^2)\Big\}\cos^2(\theta_c)$$
$$+ \Big\{-\bar{u}(x,Q^2) - \bar{d}(x,Q^2) + 2s(x,Q^2)$$
$$+ \theta(yE - W_c)\Big[\frac{1}{\eta_c}\,d(\xi_c,Q^2) + \frac{1}{\eta_c}\,u(\xi_c,Q^2)\Big]\Big\}\sin^2(\theta_c), \quad (7)$$

where θ_c is the Cabbibo angle ($\sin^2\theta_c = 0.05$) and $y = E_h/E$ is the fraction of the incoming neutrino energy delivered to the nucleon. We take the charm threshold to be $W_c = 3$ GeV and $\xi_c = x\eta_c$, $\eta_c = (1 + m_c^2/Q^2)$ with $m_c = 1.5$ GeV. The last four parameters determine the threshold of charm production. We make the usual assumptions:

1) $R_{\nu} = 0$
2) $\bar{u}(x) \equiv \bar{d}(x) \equiv \bar{s}(x) \equiv s(x)$
3) $c(x) \equiv 0$

and compare our calculated F_2^{ν} and xF_3^{ν} with their experimental values recently obtained from the CERN bubble chamber data.[10] In the region $Q^2 > 4$ GeV^2, the majority of the data was taken from BEBC with an incident neutrino energy in the range 20 - 200 GeV. Some Gargamelle data with $2 \leq E_{\nu} \leq 20$ GeV was included for $x > 0.3$ at $Q^2 = 4$ GeV^2 and $x > 0.4$ at $Q^2 = 7$ GeV^2.

Figures 21-24 show the CERN bubble chamber data and our calculated structure functions. Two curves are shown on each plot. The dashed curve is the calculation without charm production, i.e. with $\theta(yE - W_c) = 0$. The solid curve includes the effect of charm production. Most of the data in the small x region are above threshold and therefore should follow the upper curve. It should be noted that there is a 7% uncertainty in the normalization which is not included in the error bars.

In conclusion, we have shown that the quark and gluon momentum density distributions in the nucleon can be obtained using QCD and simple parton ideas. These quark momentum density distribution functions were used to calculate the form factor $F_2(x)$ for muon and electron scattering and $F_2^{\nu}(x)$ and $xF_3^{\nu}(x)$ for neutrino scattering. Reasonably good agreement with the data is shown.

We wish to thank the U. S. Department of Energy and the National Science Foundation grant #PHY77-20610 for support of this research. We would also like to thank T. Goldman for some very useful discussions.

REFERENCES

†Also at Los Alamos Scientific Laboratory, P. O. Box 1663, MS-434, Los Alamos, New Mexico 87545.

1. G.C. Fox, report to "Neutrino 78" Conference, Purdue University, April 1978, to be published.
2. H. L. Anderson, H. S. Matis and L. C. Myrianthopoulos, Phys. Rev. Lett. 40, 1061 (1978).
3. A. DeRújula, H. Georgi, and H. D. Politzer, Ann. Phys. (N.Y.) 103, 315 (1977).
4. G. C. Fox, Nuc. Phys. B131, 107 (1977).
5. A. J. Buras and K. J. F. Gaemers, Nuc. Phys. B132, 249 (1977).
6. J. Hinchliffe and C. H. Llewellyn-Smith, Nuc. Phys. B128, 93 (1977).
7. G. R. Farrar, Nuc. Phy. B77, 429 (1974).
8. R. D. Field, "Can Existing High Transverse Momentum Hadron Experiments be Interpreted by Contemporary Quantum Chromodynamic Ideas?" CALT-68-633 (1977).
9. G. C. Fox, "Application of Quantum Chromodynamics to High Transverse Momentum Hadron Production" CALT-68-643 (1978).
10. P. C. Bosetti, et al. submitted to Nucl. Phys. B; also Oxford University Report 16/78.
11. H. L. Anderson, et al., Phys. Rev. Lett. 37, 4 (1976) and 38, 1450 (1977); B. Gordon et al., submitted to Phys. Rev. Lett.; also H. L. Anderson et al., paper submitted to this Conference, "Muon Scattering at 219 GeV."
12. R. E. Taylor and W. B. Atwood; compilation of MIT-SLAC electron scattering results. H. W. Kendall and J. I. Friedman; tables of electron scattering results (A. Bodek et al., to be published).
13. W. K. Tung, Phys. Rev. D17, 738 (1978); O. Nachtmann, private communication.
14. I. Karliner and J. D. Sullivan, U. of Illinois preprint Ill-(TH)-78-20 (1978).

FERMILAB-CONF-78-129-E

TABLE I

Quark and Gluon Moments and the Value of Λ for $Q_o^2 = 10.0$ GeV^2

	n=2	n=4	n=6
⟨U + C⟩	0.332 ± 0.020	0.03557 ± 0.00049	0.00946 ± 0.00012
⟨D + C⟩	0.141 ± 0.023	0.01132 ± 0.00089	0.00228 ± 0.00022
⟨S − C⟩	0.083 ± 0.090	0.00238 ± 0.00206	0.00010 ± 0.00036
⟨G⟩	0.443 ± [illegible]	0.03974 ± 0.01166	0.00415 ± 0.00460

$\Lambda = 0.606 \pm 0.020$

TABLE II

Coefficients for the Moments of $F_2(x,Q_0^2)$ for $Q_0^2 = 10.0$ GeV^2

	n=2	n=4	n=6
M_+	0.03520	-0.001571	-0.000083
M_-	0.11905	0.015300	0.003389
M_{NS}^P	0.01831	0.003621	0.001164
M_{NS}^N	-0.04523	-0.004462	-0.001231

TABLE III

Coefficients for Quark and Gluon Distribution Functions at Various Values of Q^2 in the form $q_i(x) = (a_i + b_i x)(1-x)^{r_i}$

Q^2 (GeV^2)	Up			Down			Strange		Gluon	
	a_u	b_u	r_u	a_d	b_d	r_d	a_s	r_s	a_g	r_g
3.25	.629	2.554	2.329	.288	1.557	3.224	.581	5.023	.838	1.095
3.75	.629	2.655	2.415	.270	1.871	3.424	.575	5.118	.939	1.302
4.00	.631	2.693	2.451	.265	1.987	3.500	.572	5.160	.984	1.394
4.50	.635	2.747	2.513	.260	2.171	3.628	.567	5.234	1.067	1.561
5.50	.646	2.806	2.609	.250	2.491	3.833	.559	5.352	1.208	1.839
7.00	.664	2.831	2.710	.251	2.759	4.032	.550	5.486	1.376	2.167
9.00	.686	2.815	2.801	.260	2.966	4.210	.542	5.617	1.549	2.500
12.50	.720	2.747	2.903	.281	3.138	4.406	.533	5.776	1.773	2.925
20.00	.772	2.584	3.021	.323	3.236	4.629	.521	5.984	2.087	3.515
22.50	.785	2.534	3.047	.335	3.241	4.677	.518	6.032	2.165	3.659
40.00	.850	2.258	3.152	.400	3.152	4.872	.505	6.258	2.538	4.350
60.00	.895	2.039	3.208	.448	3.022	4.979	.498	6.404	2.796	4.822

FIGURE CAPTIONS

1. Quark and gluon momentum density distributions at $Q^2 = 3.25$ GeV^2.
2. Quark and gluon momentum density distributions at $Q^2 = 7$ GeV^2.
3. Quark and gluon momentum density distributions at $Q^2 = 20$ GeV^2.
4. Up quark distributions at various values of Q^2. The values plotted are $Q^2 = 4$, 12.5, 20, 40, and 60 GeV^2. The curve with the largest value at small x has the largest Q^2.
5. Gluon momentum density distributions. The order is the same as Figure 3.

6-10. $F_2^P(x)$ for $Q^2 = 3.25$, 9, 12.5, 22.5 GeV^2 and $\frac{1}{2}[F_2^P(x) + F_2^N(x)]$ for $Q^2 = 11.5$ GeV^2. Squares, Fermilab; crosses and triangles, MIT-SLAC.

11-15. $x^2F_2^P(x)$ for $Q^2 = 3.25$, 9, 12.5, 22.5 GeV^2 and $\frac{1}{2}[F_2^P(x) + F_2^N(x)]$ for $Q^2 = 12.5$ GeV^2. Squares, Fermilab; crosses and triangles, MIT-SLAC.

16-20. $x^4F_2^P(x)$ for $Q^2 = 3.25$, 9, 12.5, 22.5 GeV^2 and $\frac{1}{2}[F_2^P(x) + F_2^N(x)]$ for $Q^2 = 12.5$ GeV^2. Squares, Fermilab; crosses and triangles, MIT-SLAC.

21. The structure functions $F_2^\nu(x)$ and $xF_3^\nu(x)$ for neutrino data are shown at $Q^2 = 4$ GeV^2. The data are from Ref. 10. The dashed curve shows the calculation of the structure function without charm production. The solid curve shows the effect of charm production.

    a) $F_2^\nu(x)$ b) $xF_3^\nu(x)$

22. Same as Figure 21 except $Q^2 = 7$ GeV^2.
23. Same as Figure 21 except $Q^2 = 20$ GeV^2.
24. Same as Figure 21 except $Q^2 = 60$ GeV^2.

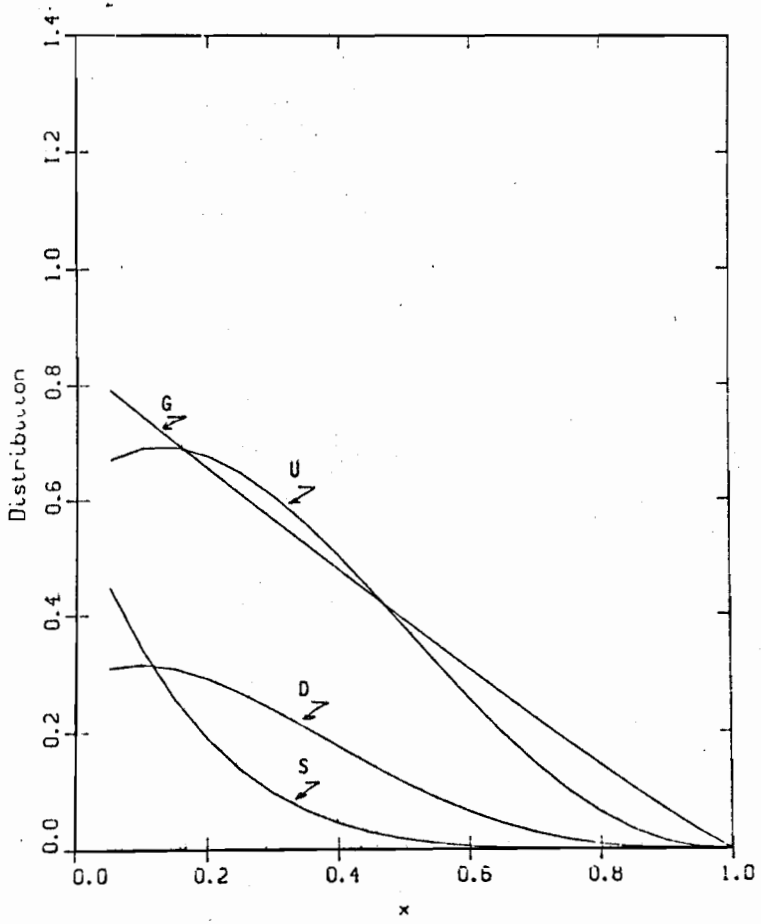

Figure 1

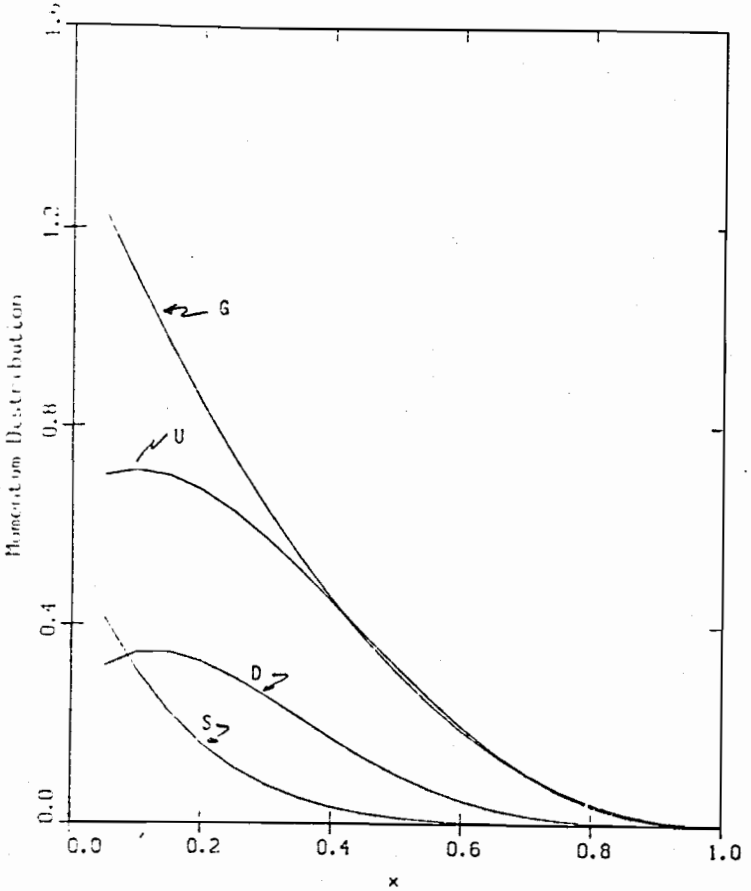

Quark and Gluon distribution at Q2 = 7 GeV ** 2

Figure 2

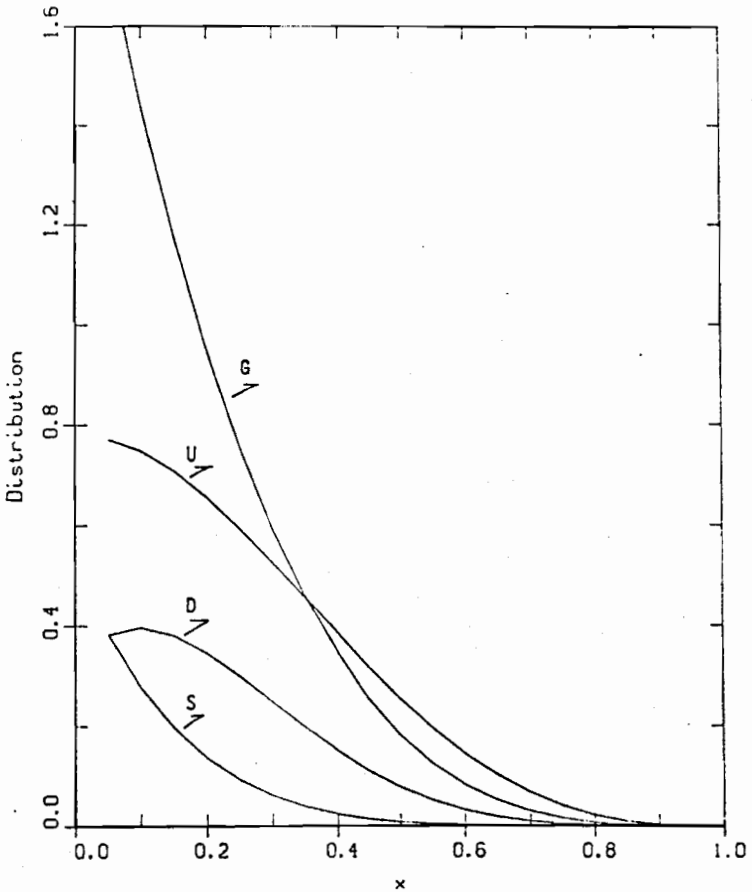

Quark and Gluon Distributions
Q2 = 20 GeV ** 2

Figure 3

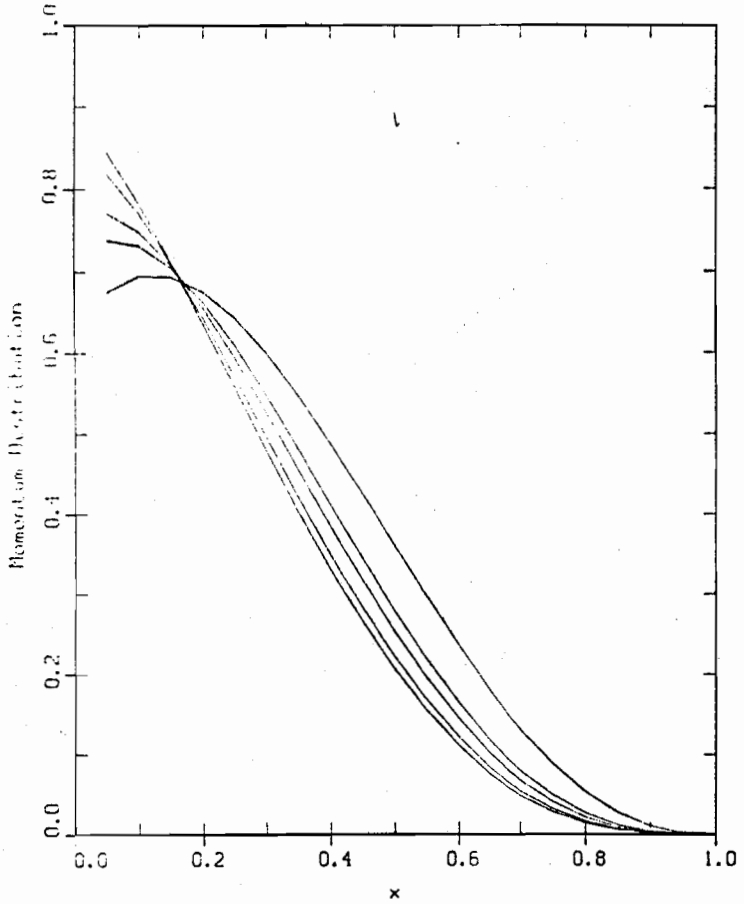

Up Quark Distribution at Q2 = 4,12.5,20,40,60 GeV xx_2

Figure 4

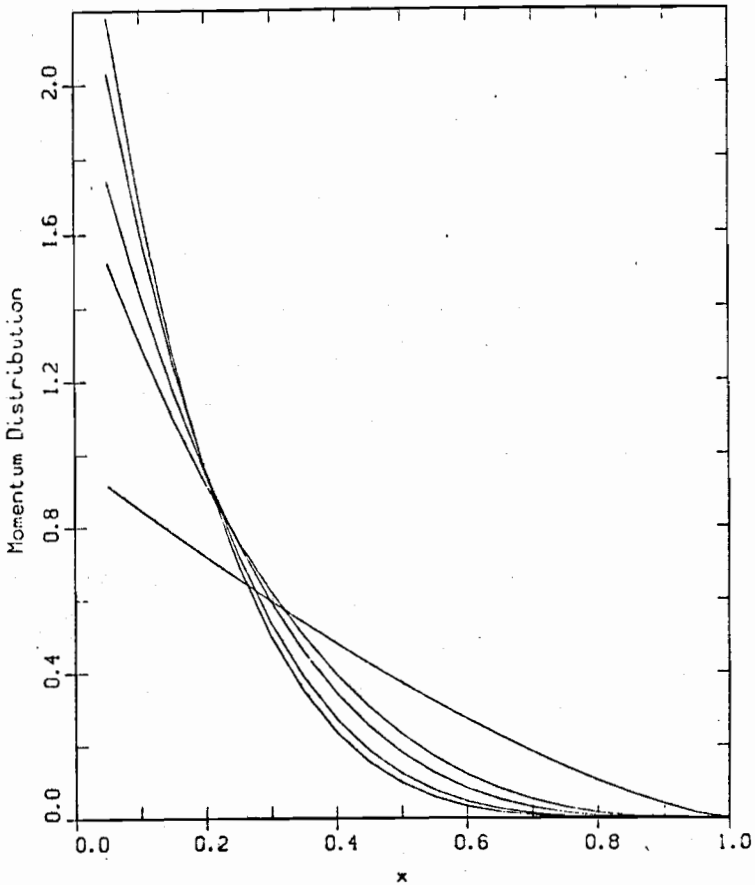

Gluon Momentum Distribution at Q2 = 4,12.5,20,40,60 GeV$xx2$

Figure 5

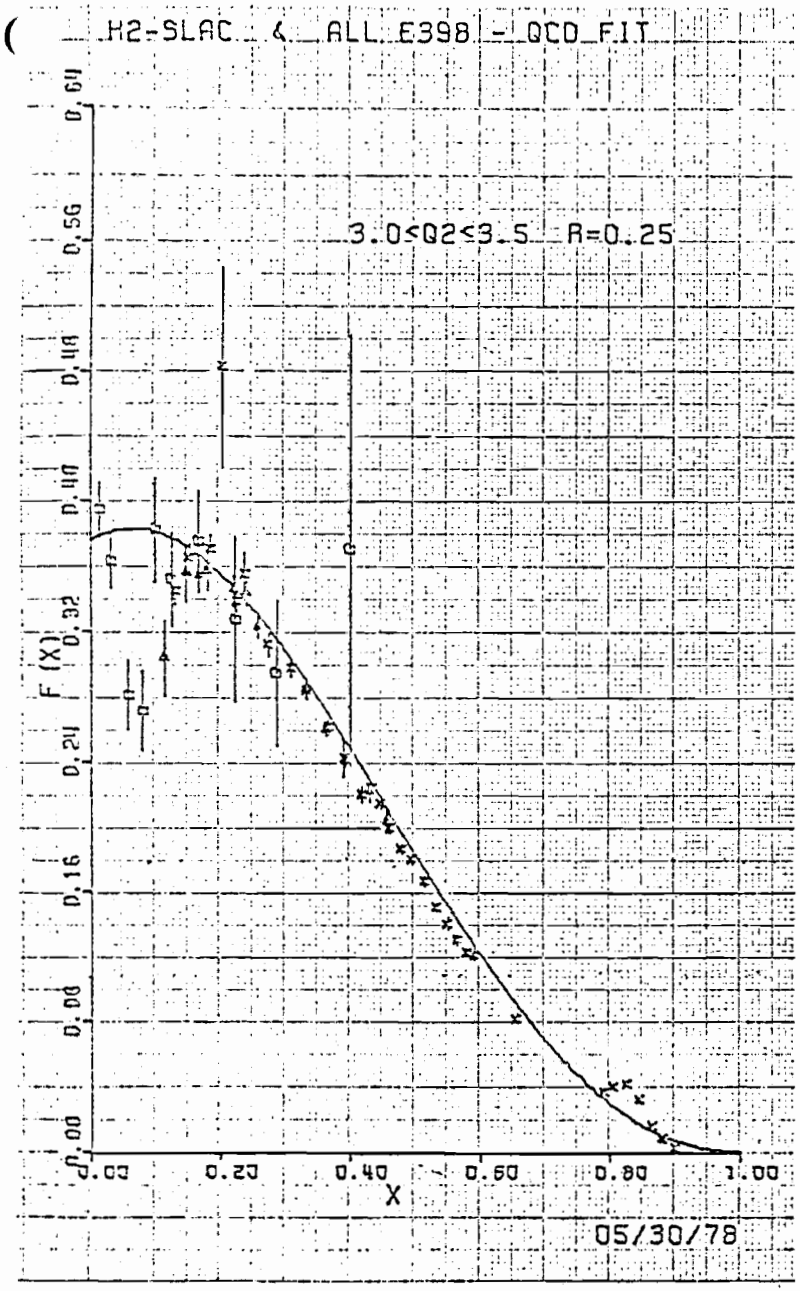

Figure 6

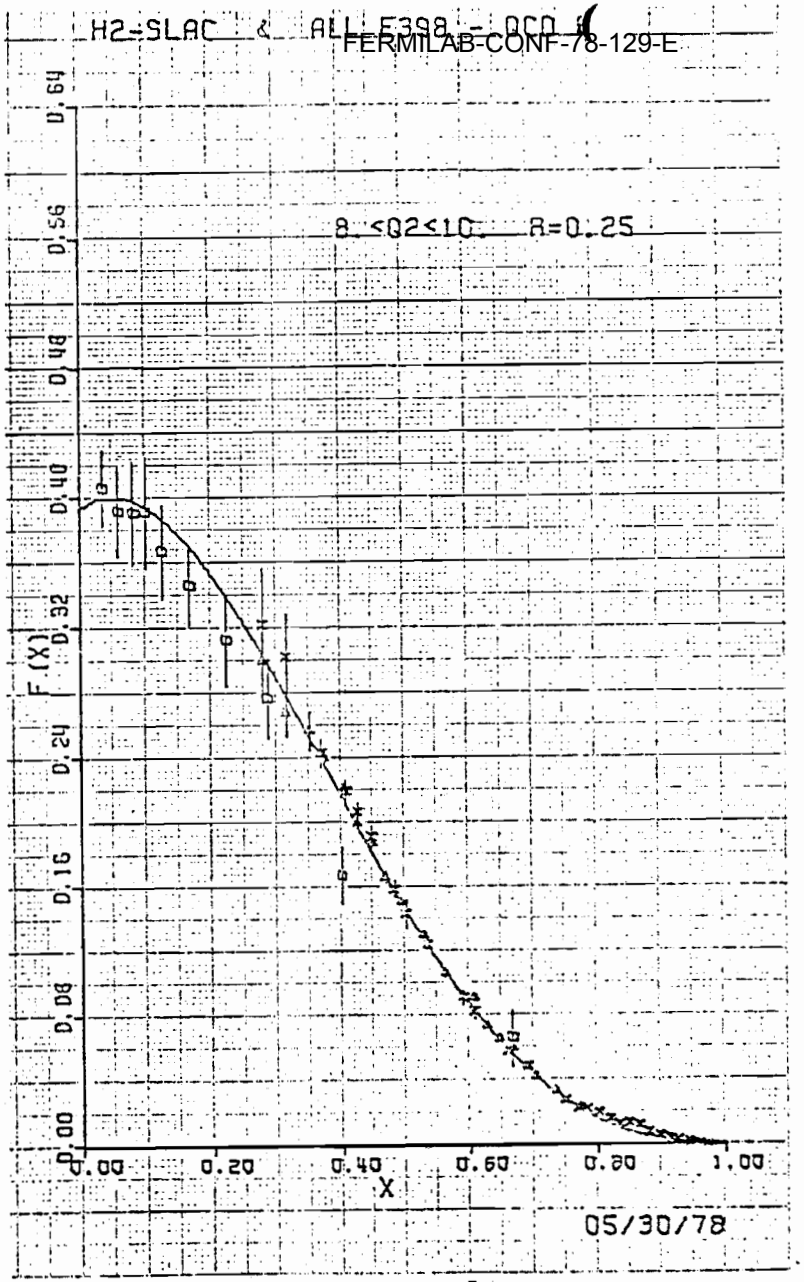

Figure 7

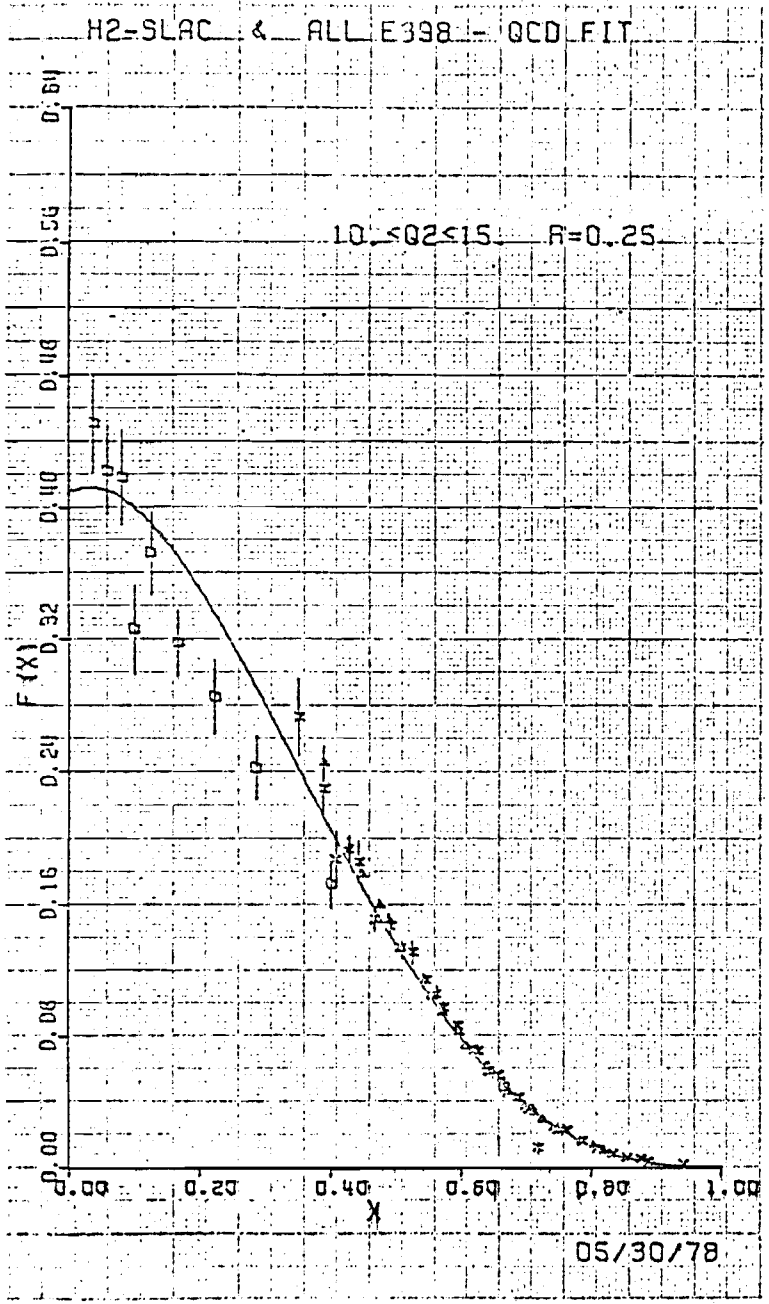

Figure 8

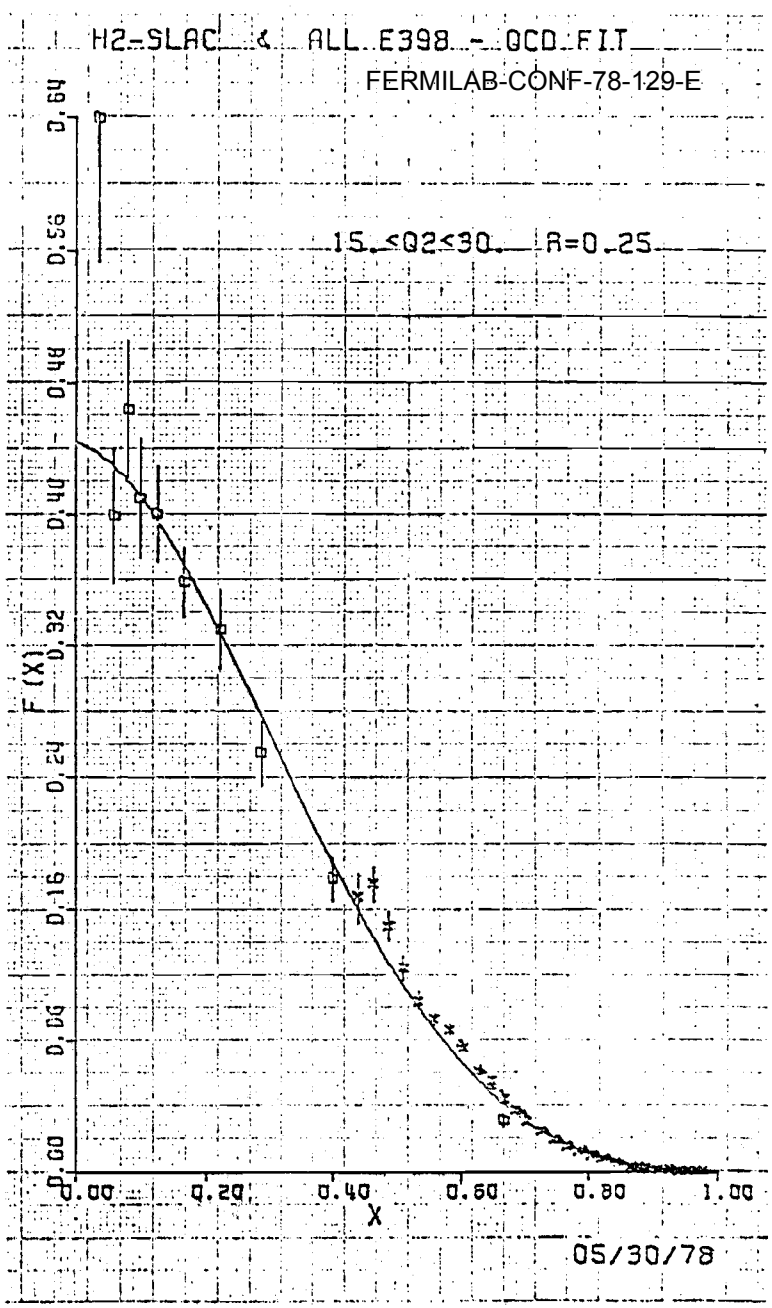

Figure 9

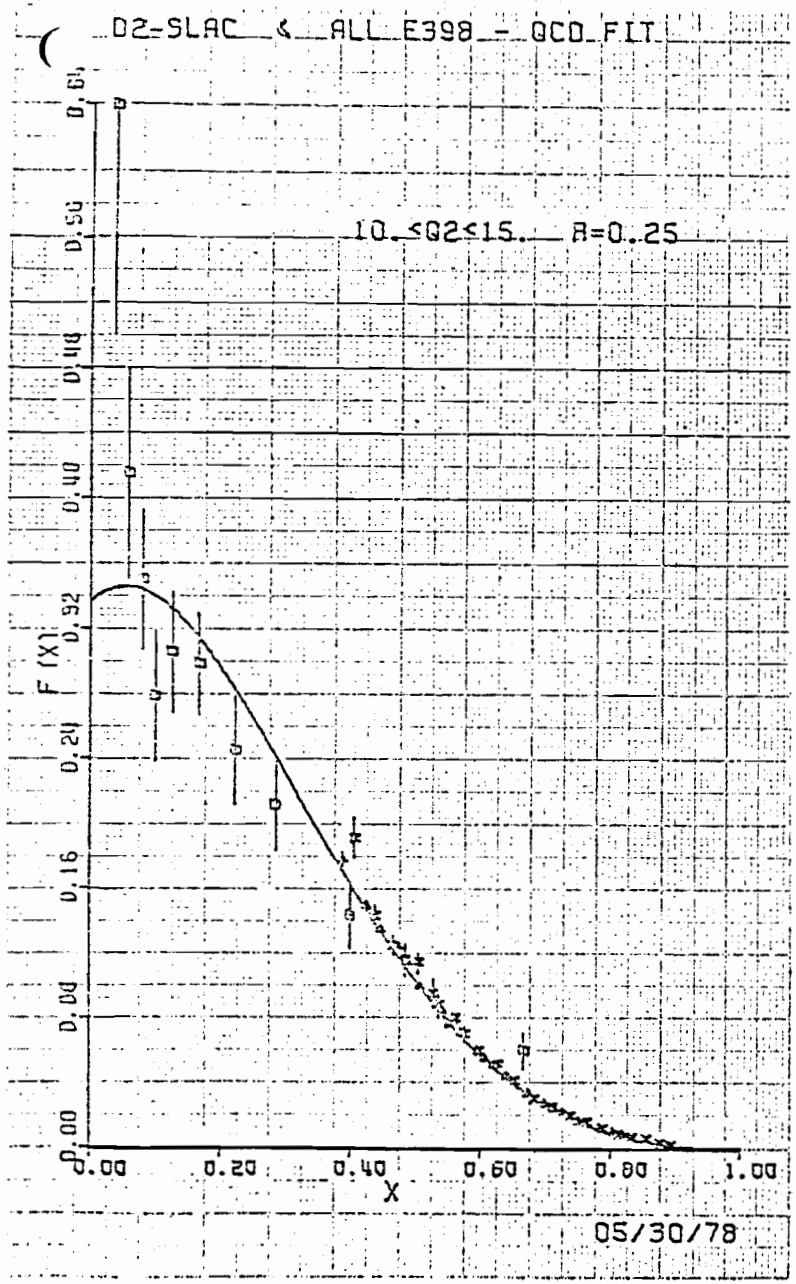

Figure 10

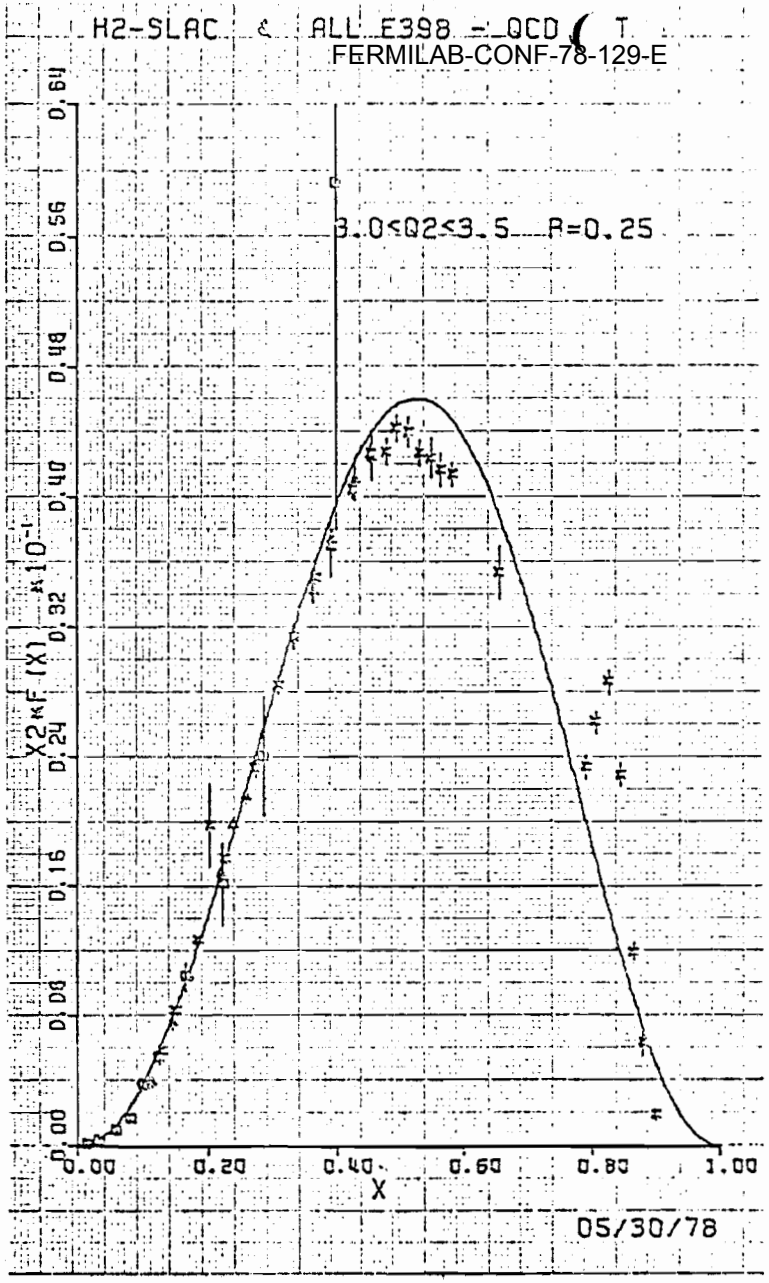

Figure 11

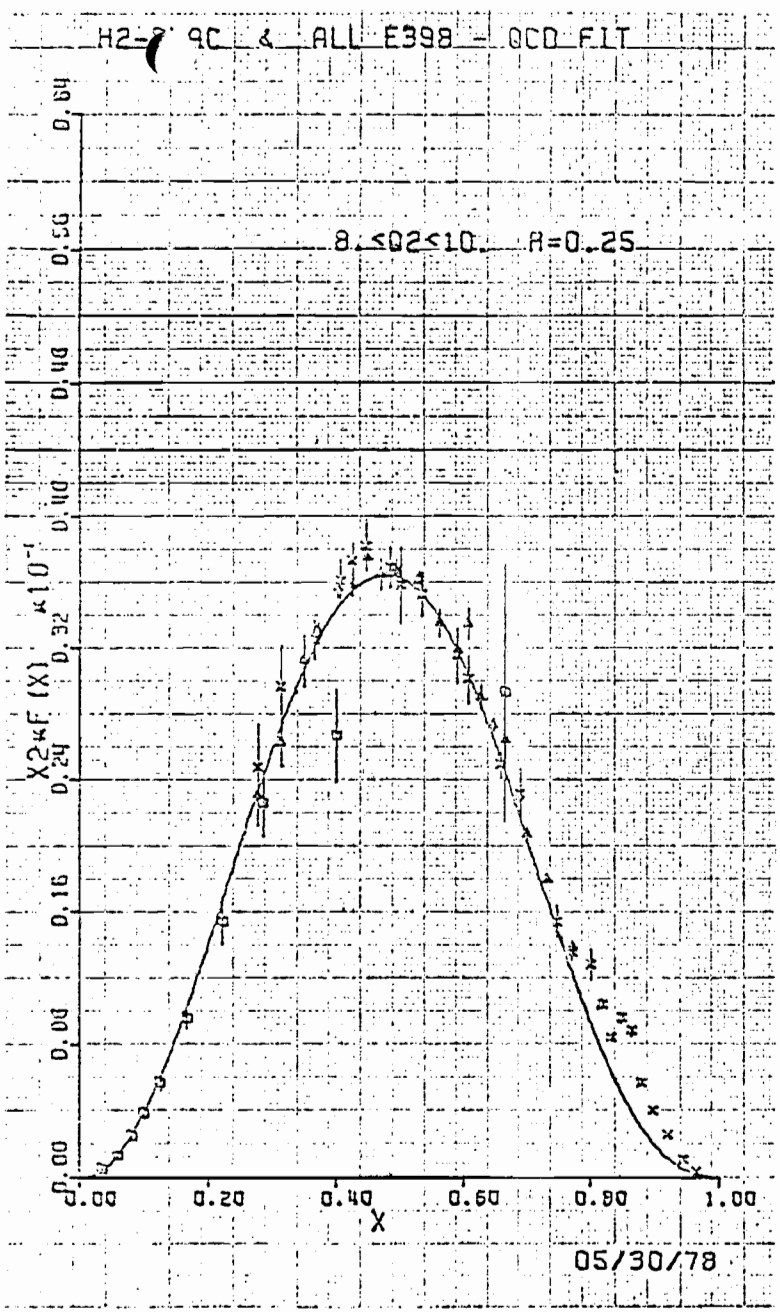

Figure 12

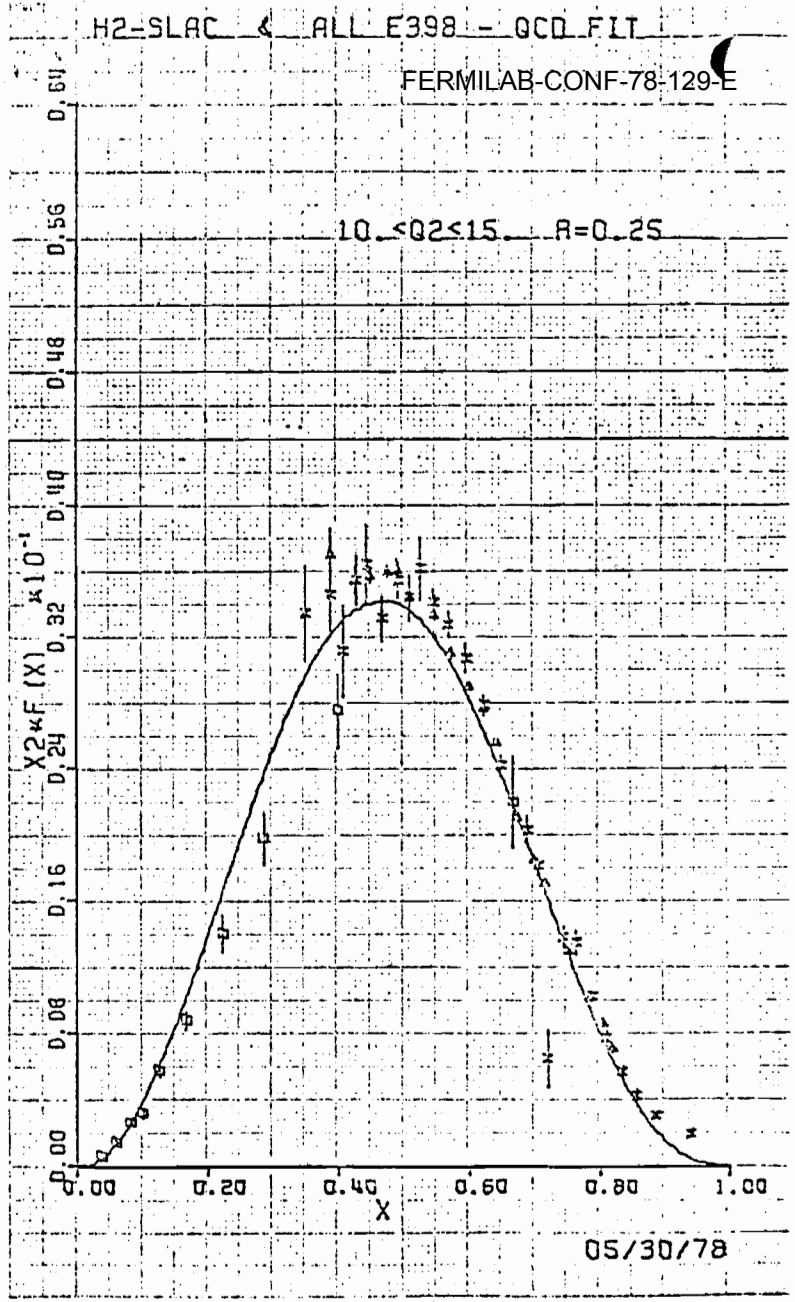

Figure 13

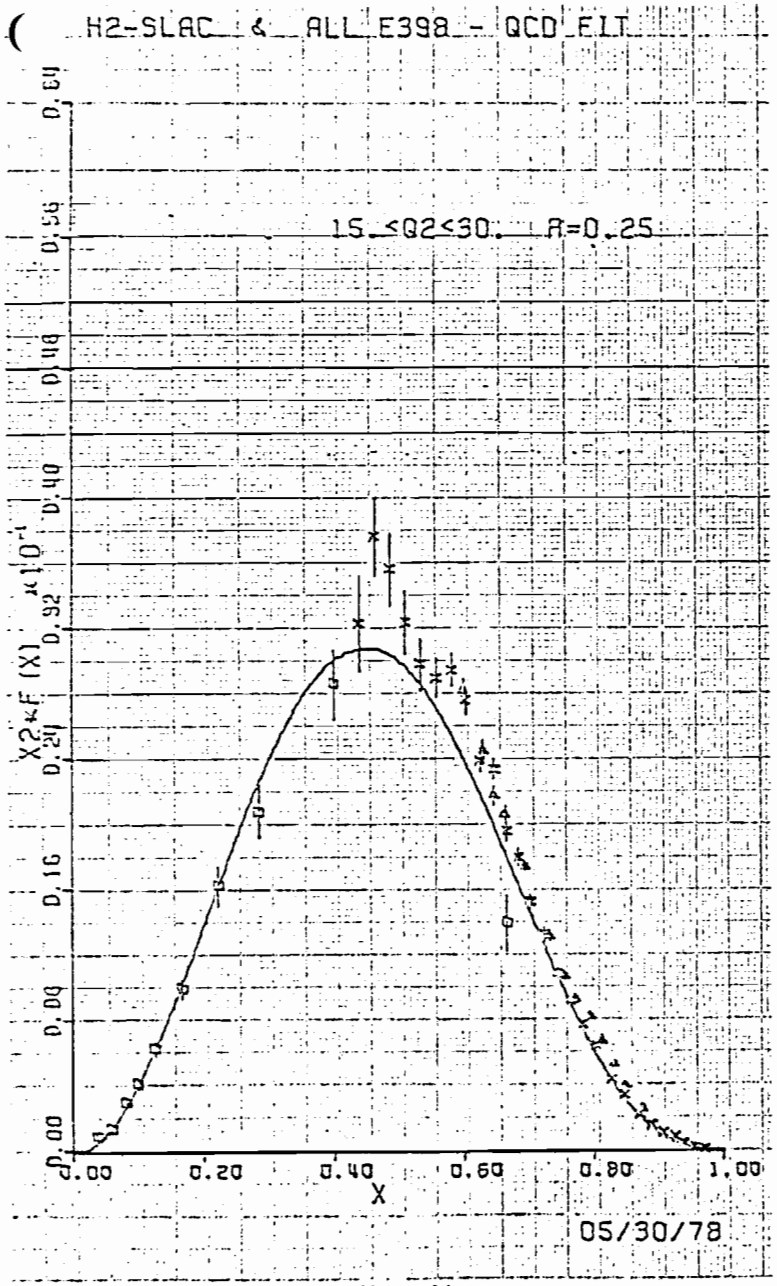

Figure 14

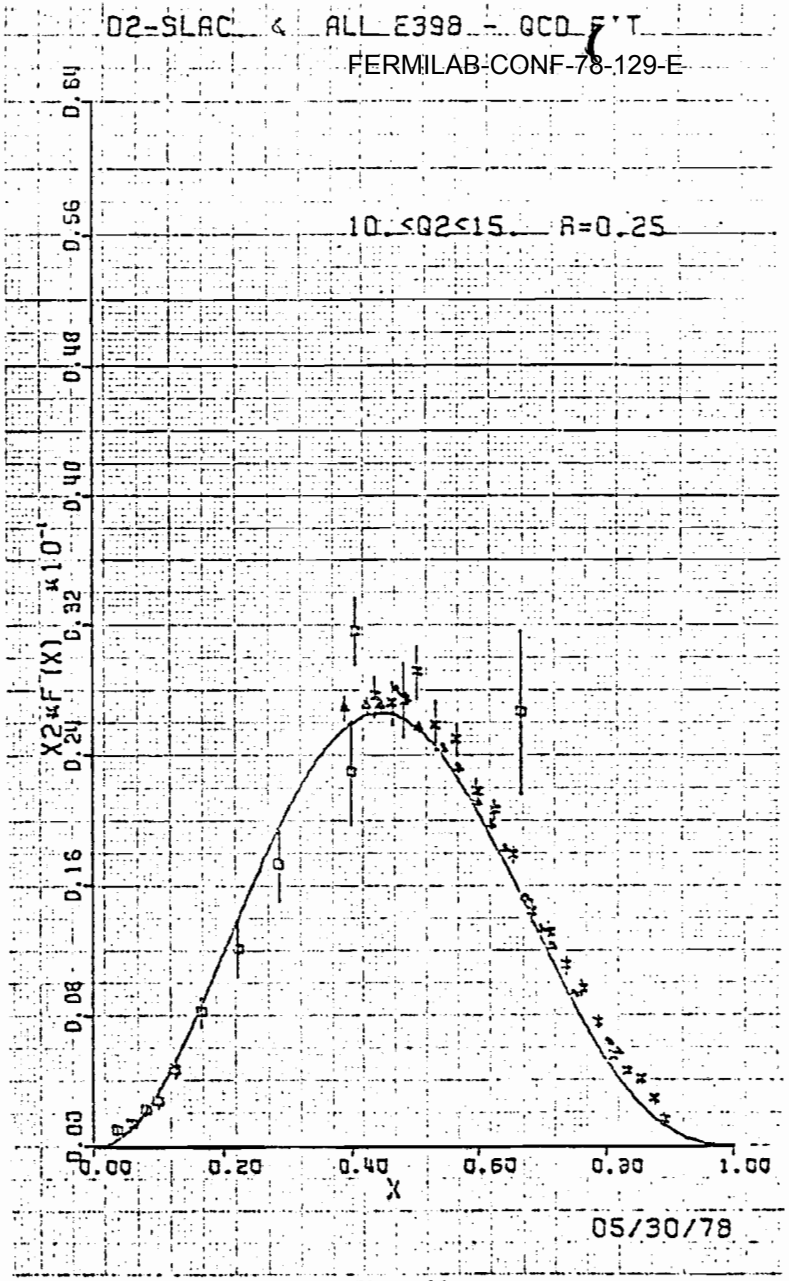

Figure 15

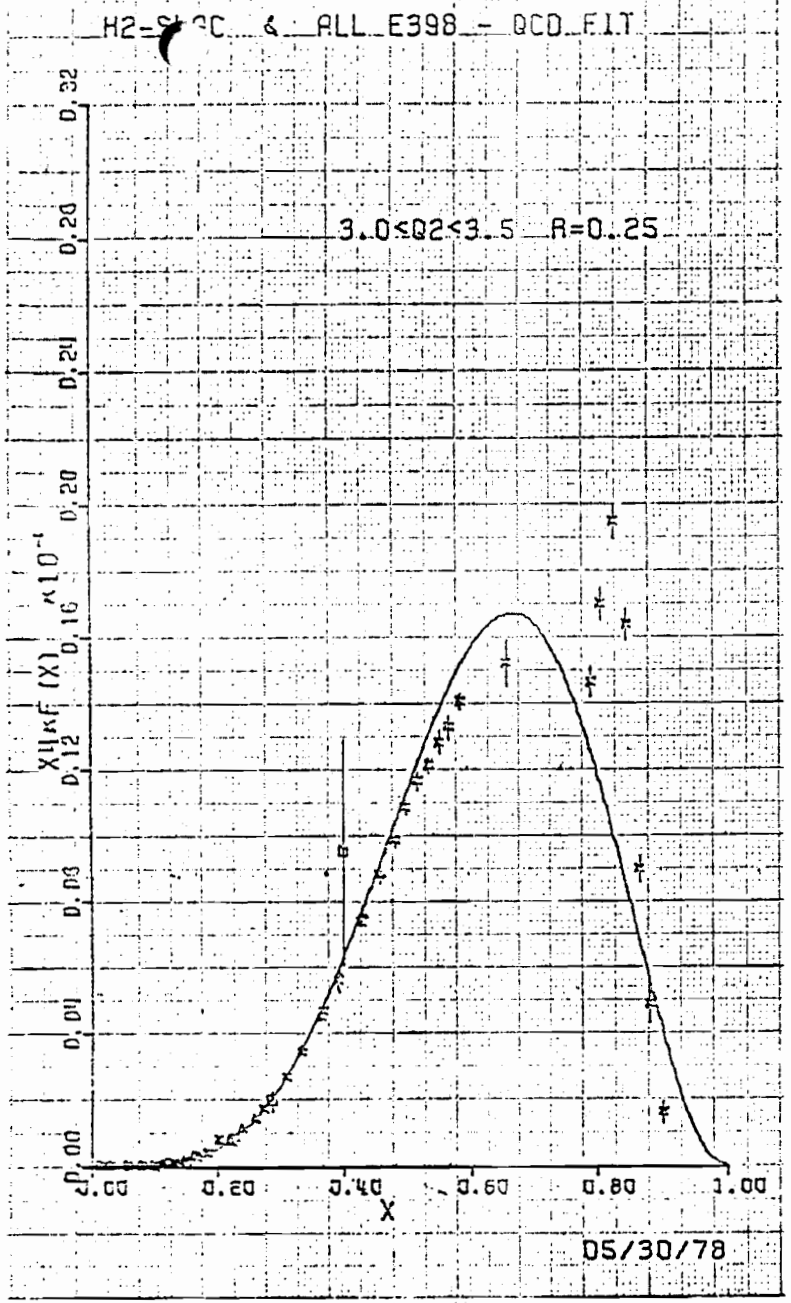

Figure 16

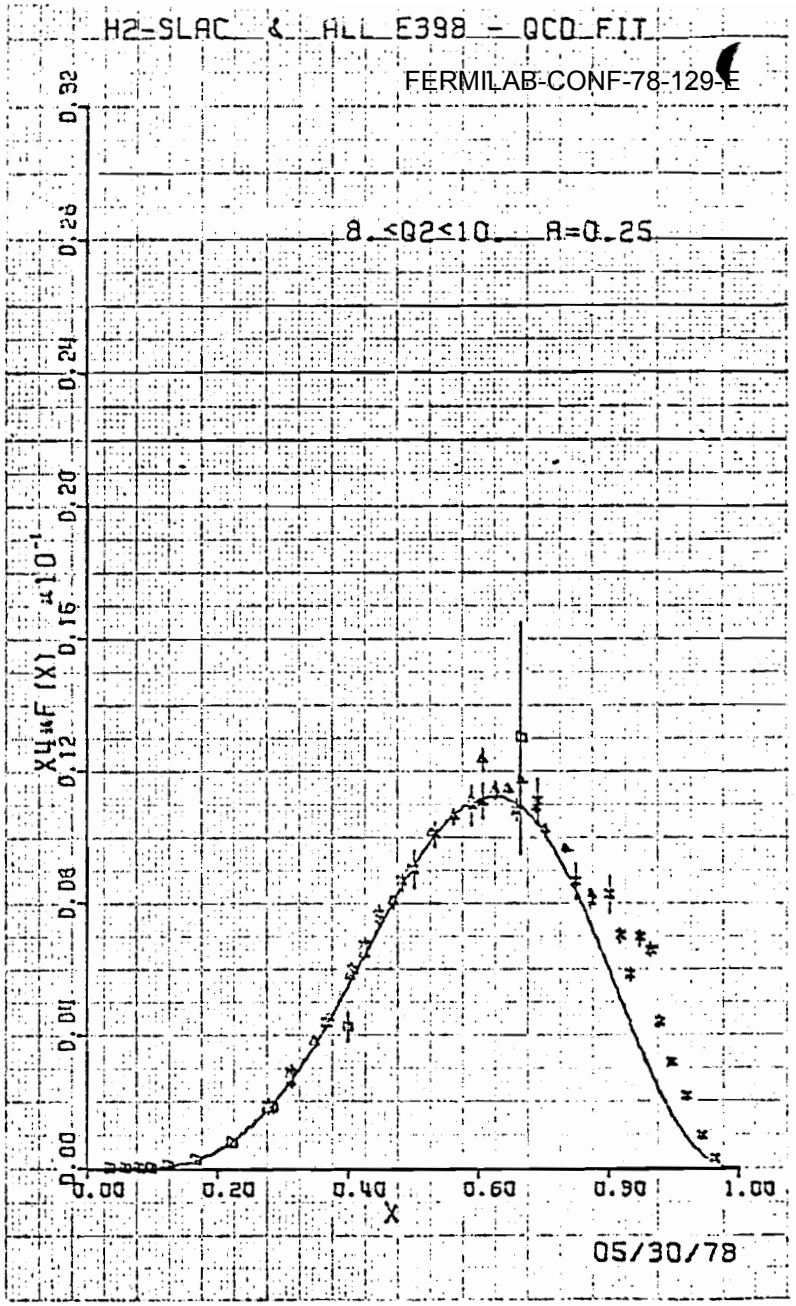

Figure 17

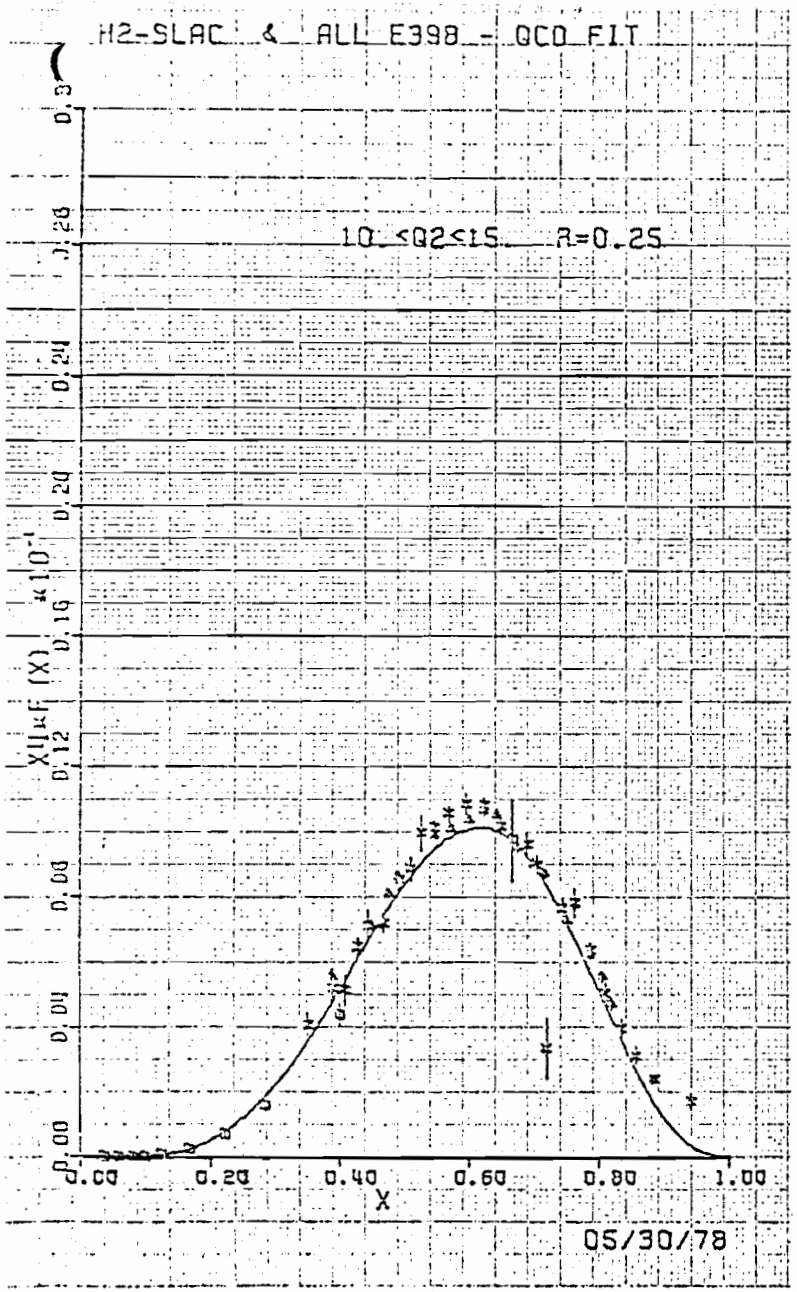

Figure 18

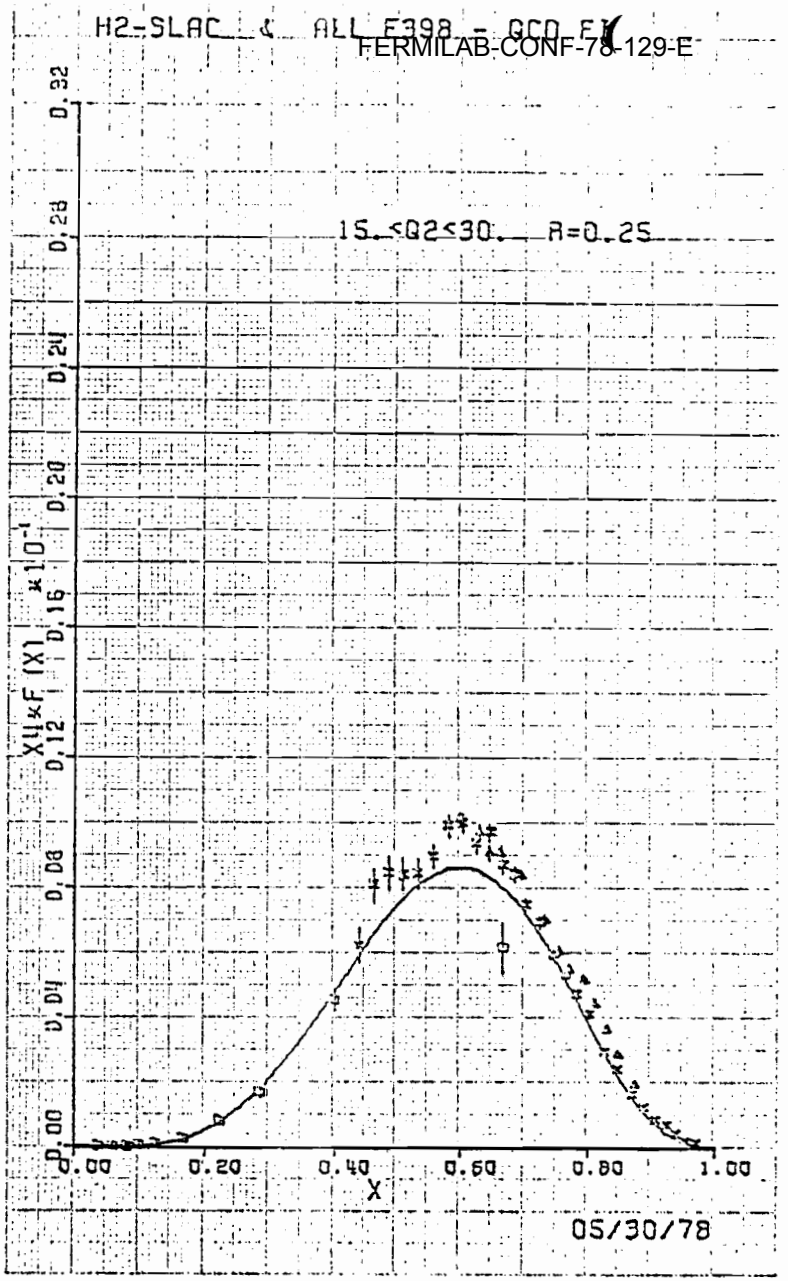

Figure 19

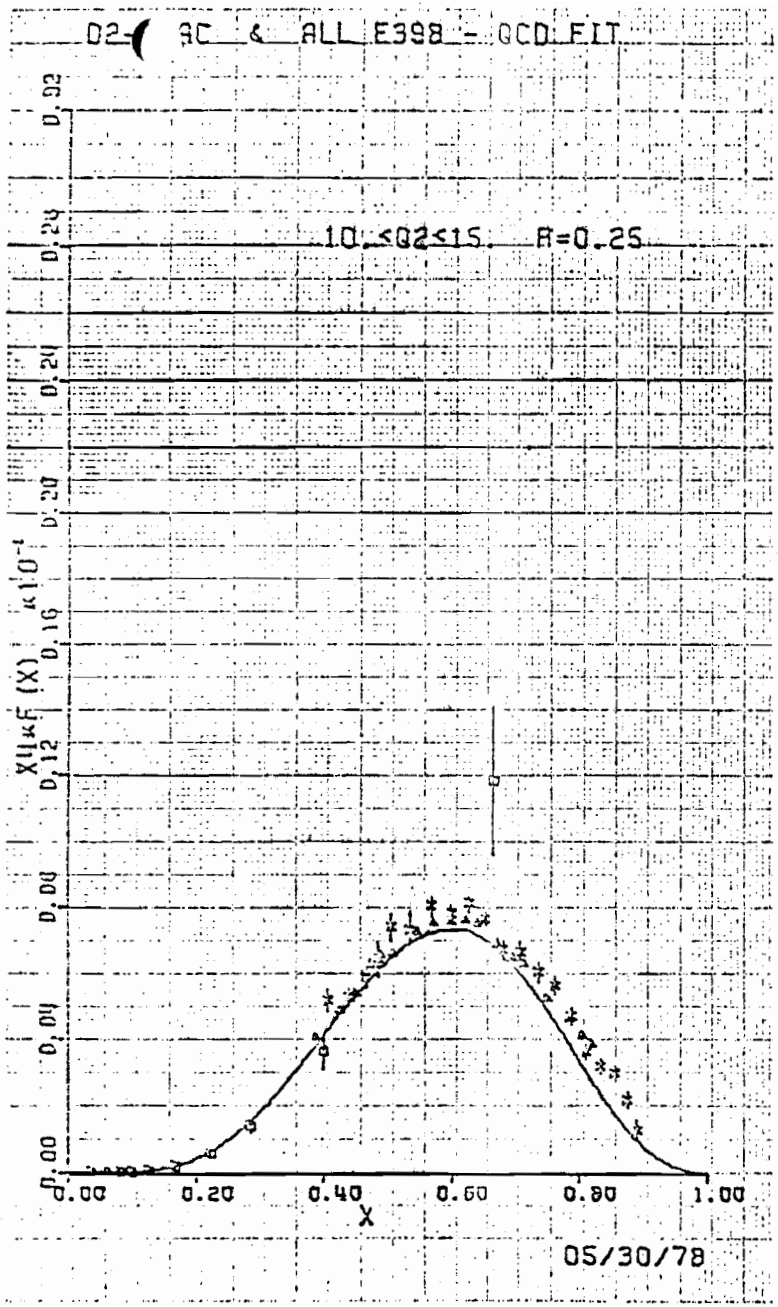

Figure 20

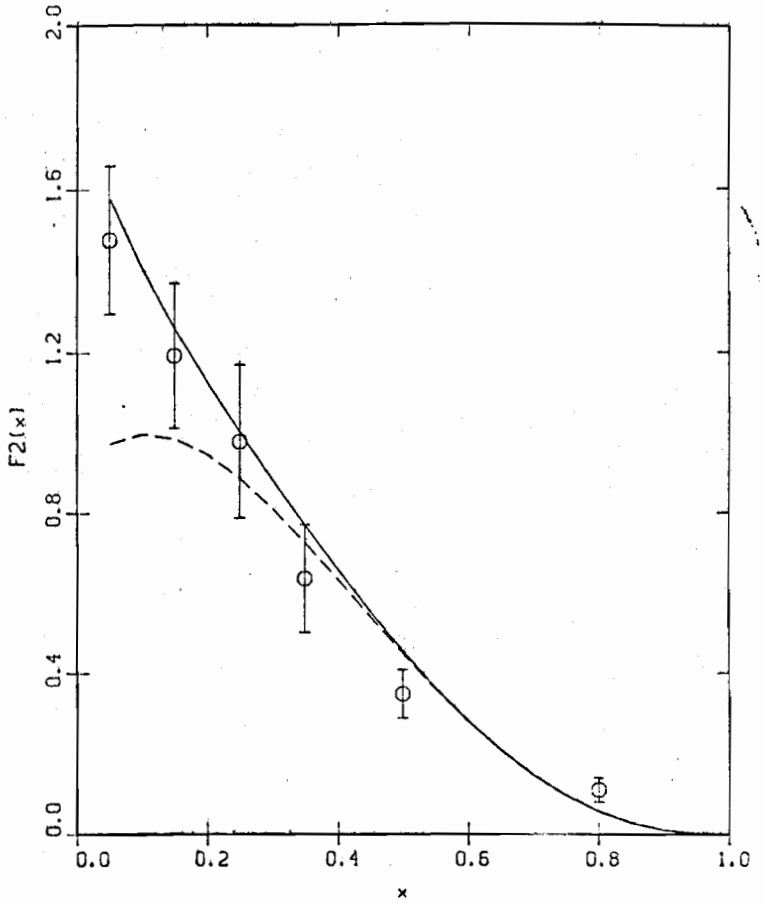

F2(x) for Neutrino Scattering
Q2 = 4.0 GeV××2

Figure 21a

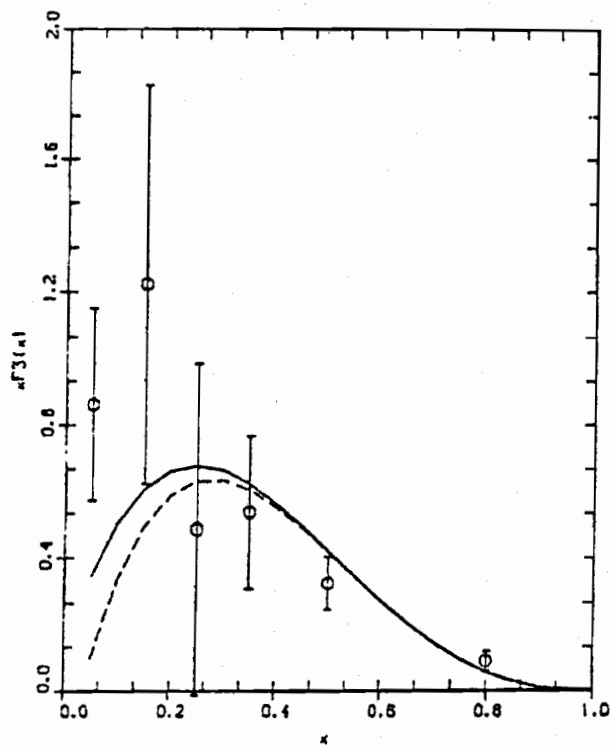

xF3(x) for Neutrino Scattering
Q2 = 4.0 GeV**2

Figure 21b

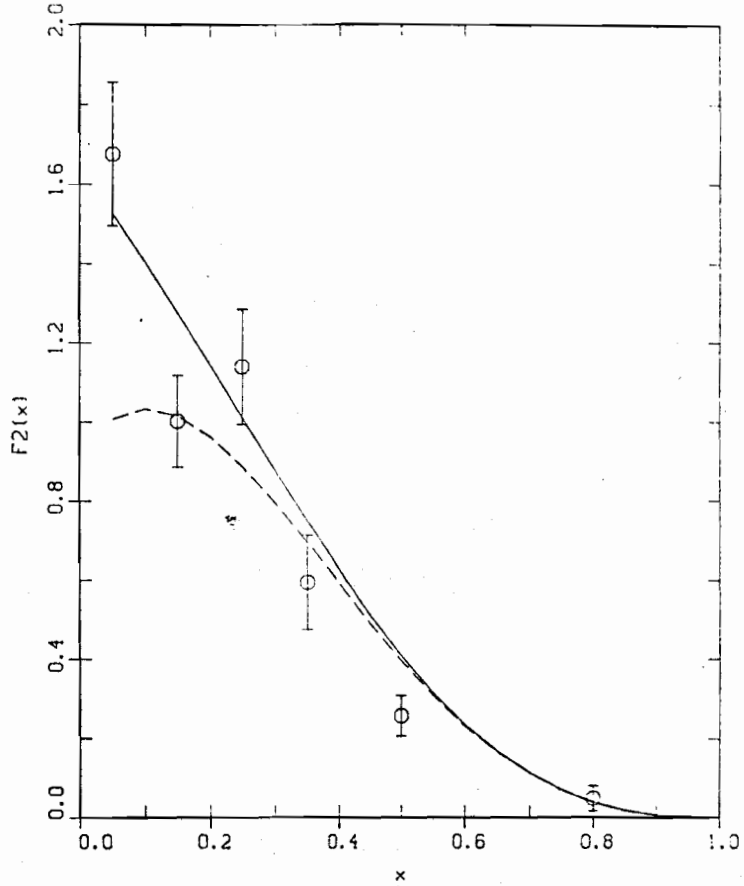

F2(x) for Neutrino Scattering
Q2 = 7.0 GeV**2

Figure 22a

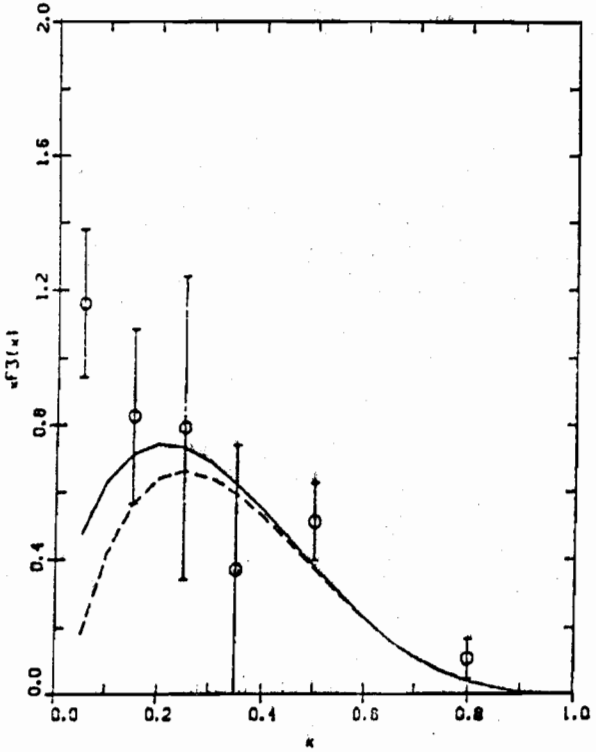

xF3(x) for Neutrino Scattering
Q2 = 7 GeV××2

Figure 22b

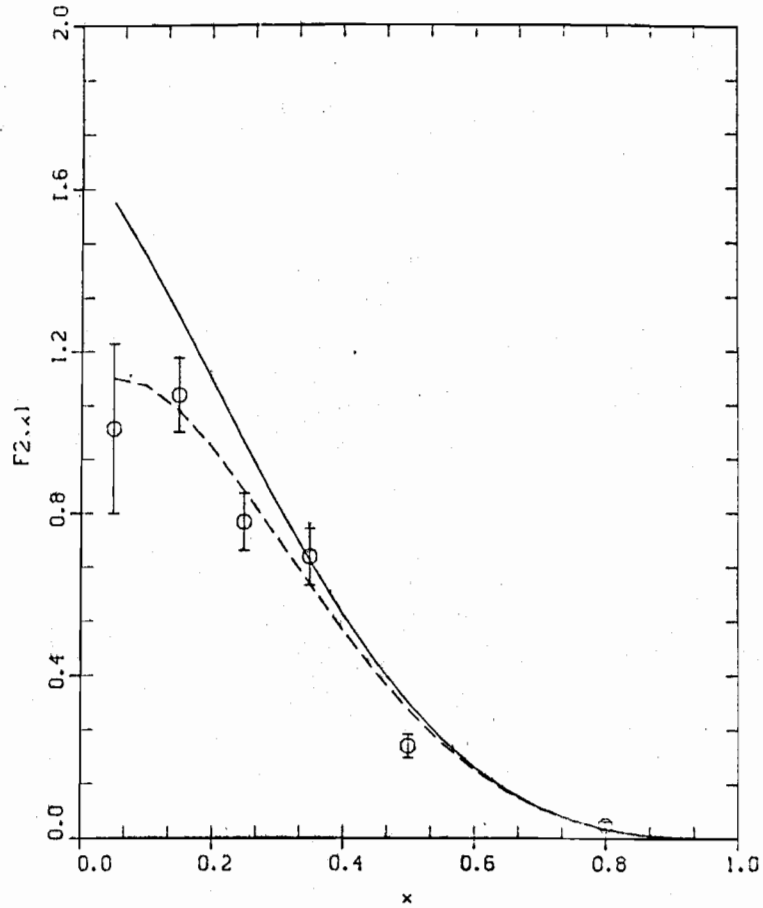

F2(x) for Neutrino Scattering
Q2 = 20.0 GeV ×× 2

Figure 23a

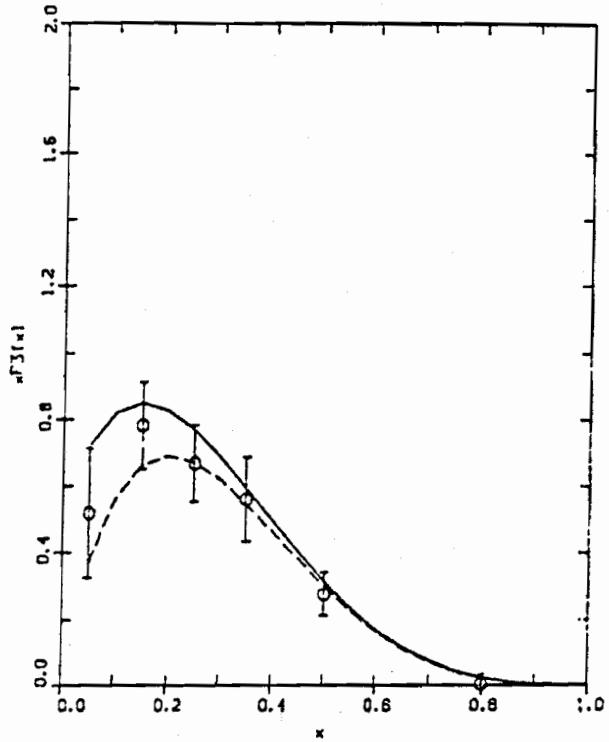

xF3(x) for Neutrino Scattering
Q2 = 20 GeV××2

Figure 23b

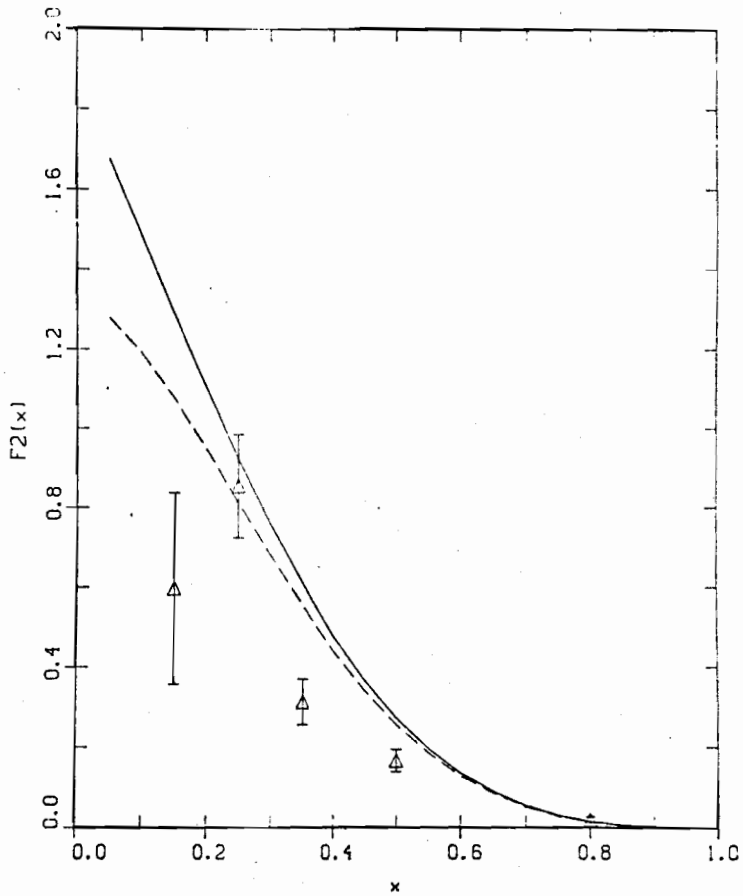

F2(x) for Neutrino Scattering
Q2 = 60 GeV ×× 2

Figure 24a

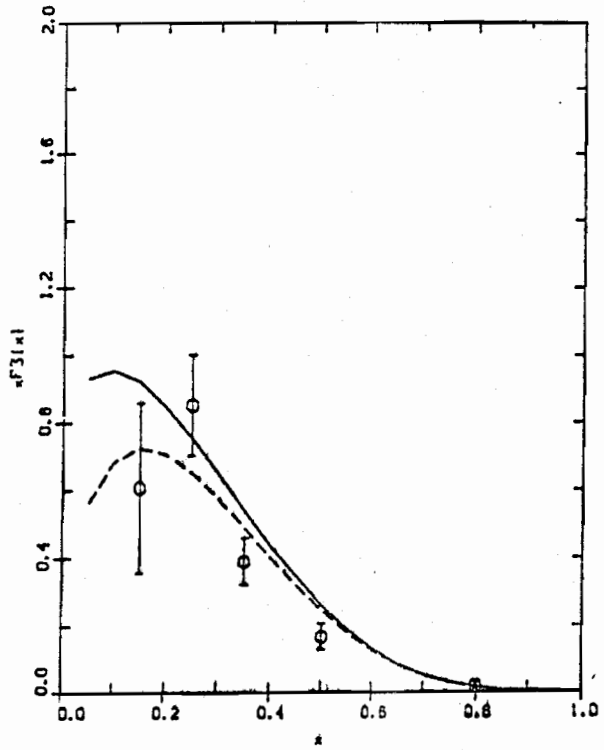

xF3(x) for Neutrino Scattering
Q2 = 60 GeV**2

Figure 24b